

Fig. S1 XRD pattern of the as-prepared V<sub>2</sub>O<sub>5</sub>.xH<sub>2</sub>O nanosheets/RGO nanocomposite before annealing

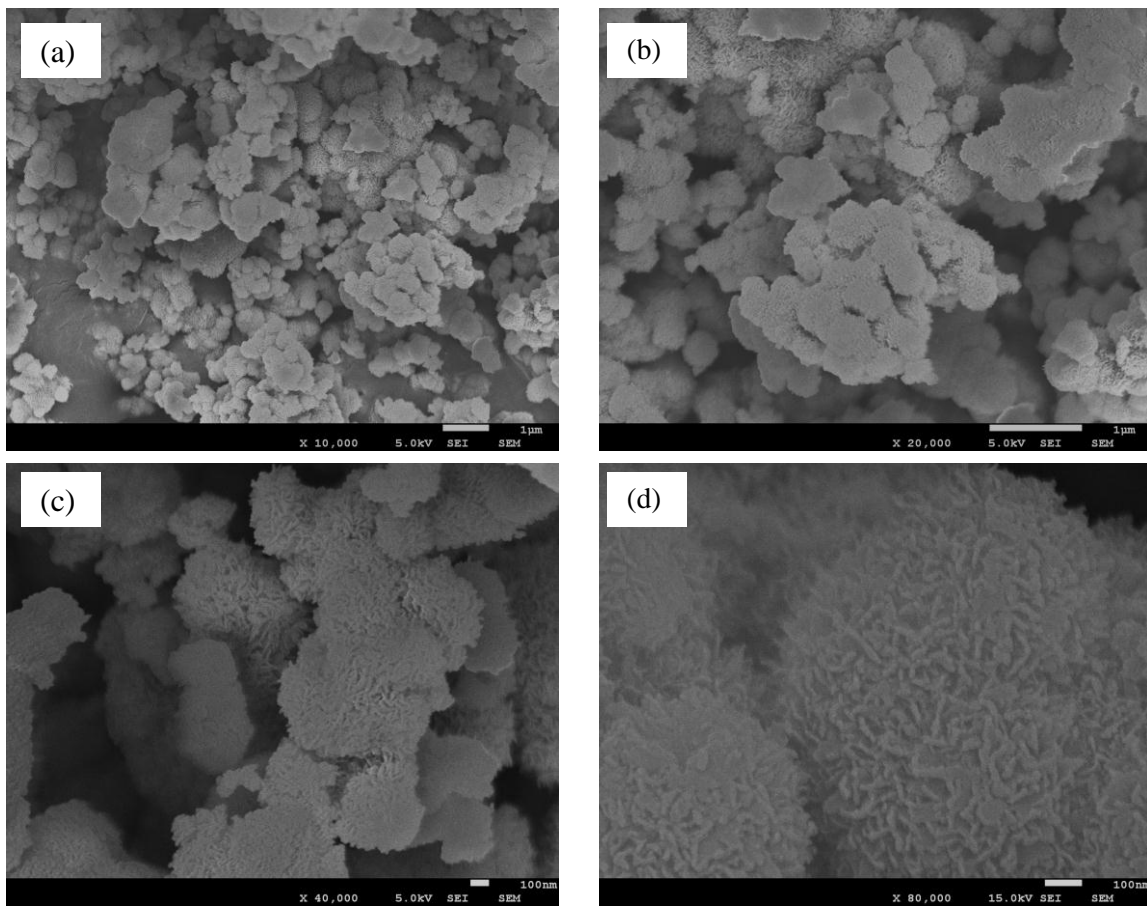


Fig. S2 SEM images of V<sub>2</sub>O<sub>5</sub> microspheres at different magnifications

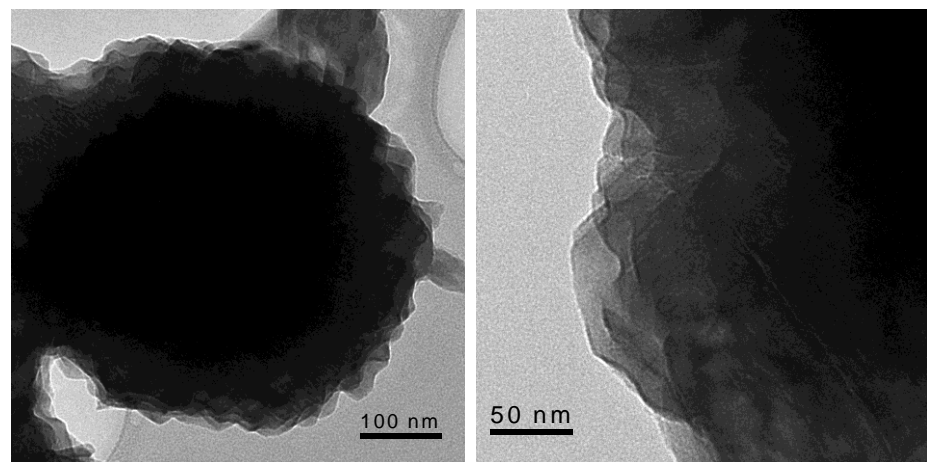


Fig. S3 TEM images of V<sub>2</sub>O<sub>5</sub> microspheres at different magnifications

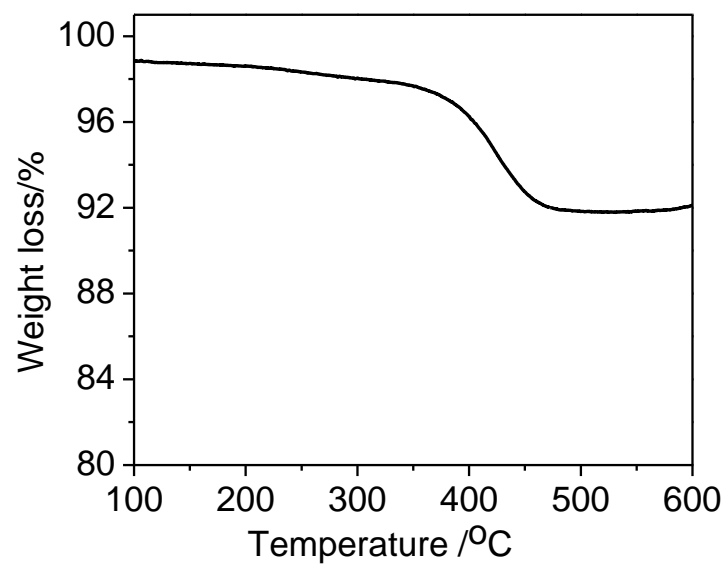


Fig. S4 Thermogravimetric analysis of V<sub>2</sub>O<sub>5</sub> nanosheets/RGO nanocomposite

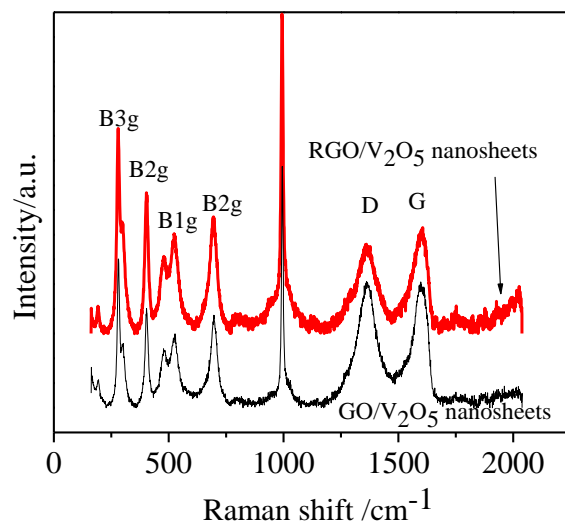


Fig. S5 Raman spectra of  $\text{V}_2\text{O}_5$  nanosheets/RGO nanocomposite (red) and  $\text{V}_2\text{O}_5$  nanosheets/GO nanocomposite (black)

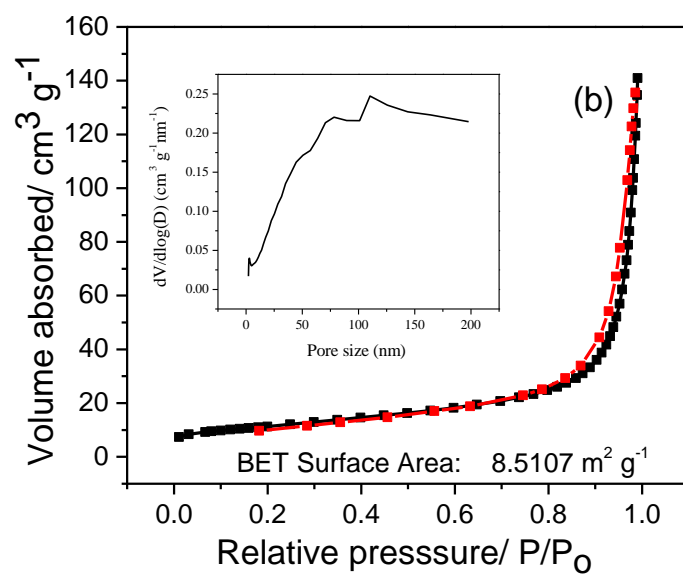
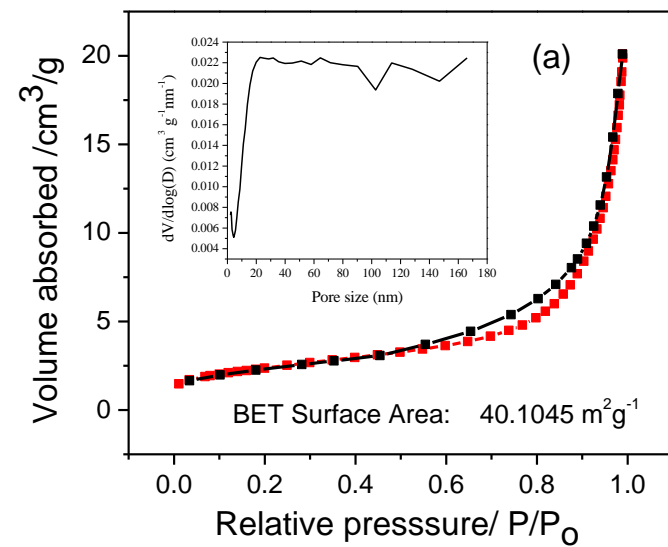


Fig. S6 Nitrogen adsorption and desorption isotherm (the insets show the pore size distribution) of V<sub>2</sub>O<sub>5</sub> nanosheets/RGO nanocomposite (a) and pure V<sub>2</sub>O<sub>5</sub> microsphere (b)

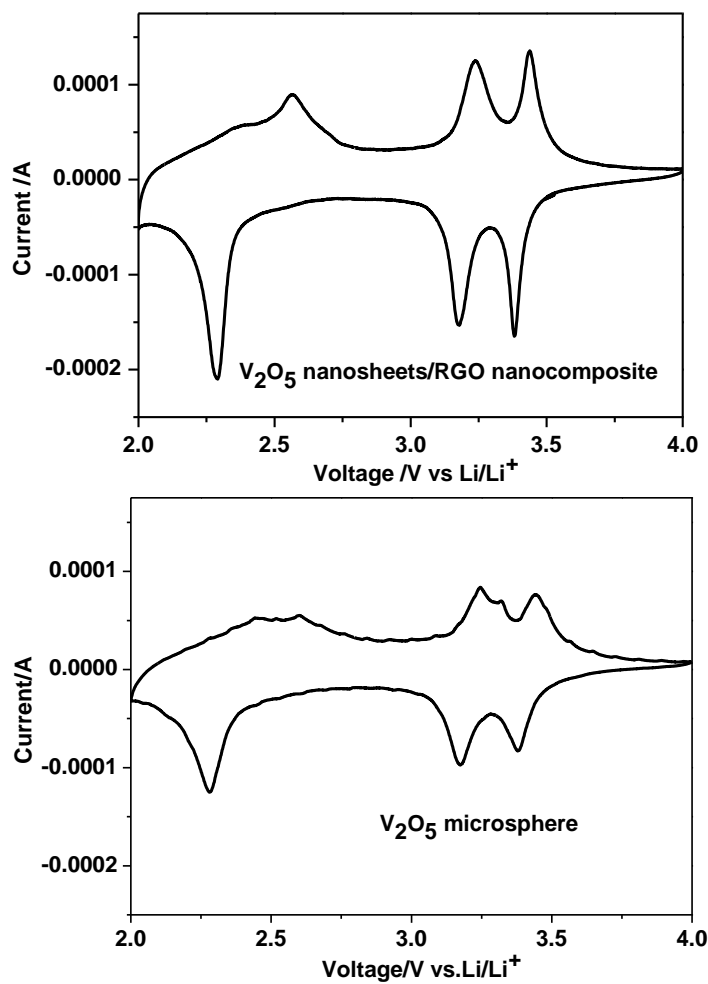


Fig. S7 Cyclic voltammograms of  $\text{V}_2\text{O}_5$  nanosheets/RGO nanocomposite and  $\text{V}_2\text{O}_5$  microsphere electrode at a scan rate of  $0.1 \text{ mV s}^{-1}$

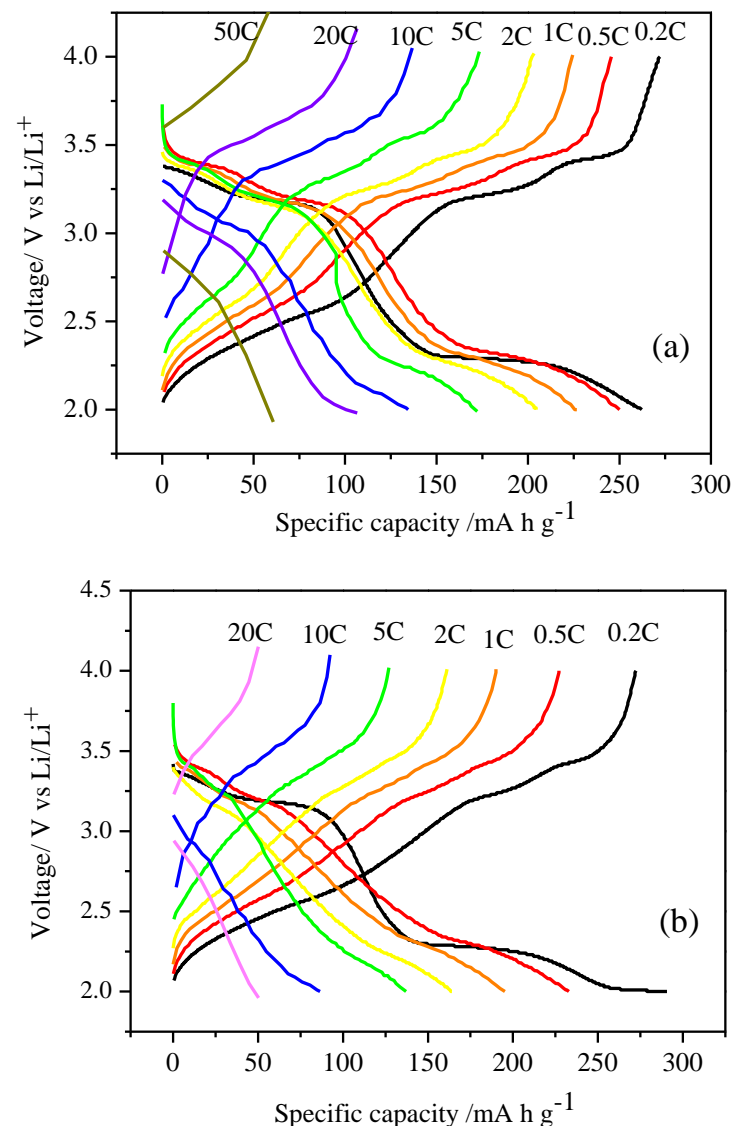


Fig.S8 Charge/discharge profiles of V<sub>2</sub>O<sub>5</sub> nanosheets/RGO nanocomposite electrode (a) and V<sub>2</sub>O<sub>5</sub> microsphere electrode (b) at different current rates.

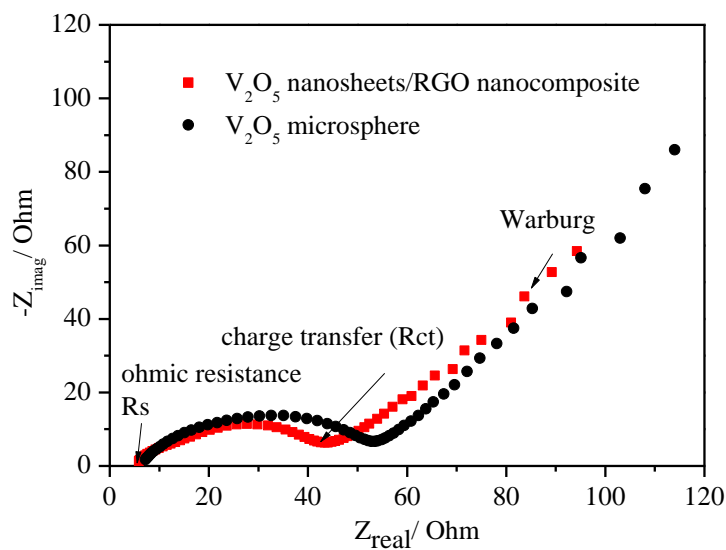


Fig. S9 Nyquist plots of the  $\text{V}_2\text{O}_5$  nanosheets/RGO nanocomposite electrode and  $\text{V}_2\text{O}_5$  microsphere electrodes after 5 charge/discharge cycles.